JACS
JOURNAL OF THE AMERICAN CHEMICAL SOCIETY
Article
pubs.acs.org/JACS

Peptide-Mediated Nanoengineering of Inorganic Particle Surfaces: A General Route toward Surface Functionalization via Peptide Adhesion Domains

Thorsten Schwemmer,[†,‡] Jens Baumgartner,[§] Damien Faivre,[§] and Hans G. Börner*[,†]

[†]Humboldt-Universität zu Berlin, Department of Chemistry, Laboratory for Organic Synthesis of Functional Systems, Brook-Taylor-Strasse 2, D-12489 Berlin, Germany

[‡]Center of Supramolecular Interactions Berlin (CSI Berlin) at Freie-University Berlin, Berlin, Germany

[§]Max Planck Institute of Colloids and Interfaces (Department of Biomaterials), 14424 Potsdam, Germany

Supporting Information

ABSTRACT: The peptide-mediated functionalization of inorganic particle surfaces is demonstrated on gadolinium oxide (GdO) particles, revealing specific means to functionalize nano- or microparticles. Phage display screening is exploited to select 12*mer* peptides, which exhibit sequence-specific adhesion onto surfaces of GdO particles. These peptide adhesion domains are exploited to effectively decorate GdO particles with fluorescently labeled poly(ethylene oxide) (PEO), proving to result in a stable surface modification as shown by significant reduction of protein adsorption by 80%, compared to nonfunctionalized particles. Peptide adhesion and stability of the noncovalent coating are investigated by adsorption/elution experiments and Langmuir isotherms. Fluorescence microscopy, contact angle, and energy dispersive X-ray (EDX) measurements confirmed the sequence specificity of the interactions by comparing adhesion sequences with scrambled peptide sequences. Noncovalent, but specific modification of inorganic particle surfaces represents a generic strategy to modulate functionality and function of nano- or microparticle surfaces.

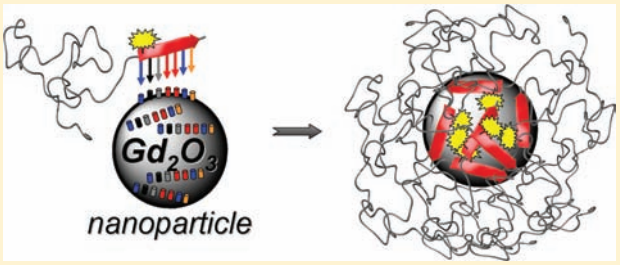

INTRODUCTION

In the recent decades inorganic nano- or submicroparticles (NPs) have received tremendous attention.[1−7] Optic, electronic, or magnetic quantum size effects, as well as large specific surface areas, and high energy surfaces were recognized as properties of nanoscaled inorganics.[8−11] These make NPs useful for broad spectra of applications, ranging from catalysts, to sensors, to coatings, to hybrid materials, optomaterials, and biomedical probes.[12−17] The functionalities present on the surfaces of particles have been identified as one key parameter, which determines for example colloidal stability, bioactivity, or compatibility. Advanced functions could also be implemented such as directed self-assembly, stimuli responsiveness, or biotargeting.[18−22] Thus, nanoengineering of NP-surfaces has become a highly important field of research.[23] Diverse functionalization routes have been investigated. Approaches range from adsorption to polymerization strategies and use methods from secondary Stöber coating, to layer-by-layer adsorption, to (mini)emulsion.[24−29] A large fraction of the studies focus on gold NPs.[30] This reflects the facts that gold NPs can be easily prepared and surface functionalization frequently exploits convenient gold−thiol interactions. The gold−thiol bond provides strong, rather surface-specific interactions and tolerates diverse functionalities.[31,32] Despite the fact that the scope of gold appears to be limited compared to the variety of other functional inorganics for example Co, TiO_2, SnO, CdS, Gd_2O_3, Fe_3O_4, MgF_2, or indium tin oxide etc., the ease of surface functionalization makes gold NPs important systems. However, generic means to selectively or even specifically modify surfaces of various inorganic NPs are mandatory.

Biologically occurring proteins like ovocleidin, osteocalcin, or sialoprotein bind specifically to distinct inorganic surfaces.[33,34] Thus, tailor-made peptide−polymer conjugates[35−38] with monodisperse peptide segments and precisely adjustable interaction capabilities[39,40] offer a generic route to surface functionalization of NPs by peptide adhesion domains (Figure 1).[41−44] So far, peptides of peptide−polymer conjugates were either adapted from protein sections or designed in rational or empirical manner. Combinatorial means have not been employed to assist bioconjugate design. Taking into account for example that 12*mer* peptides, which are composed of the 20 natural amino acids, span a sequential space of 4×10^{15} variations, combinatorial screening tools are required to select suitable candidates for NP binding. Phage display has been successfully adapted from molecular biology to material sciences.[45−49] Phage display allows selecting peptides that

Received: November 8, 2011
Published: December 23, 2011

   dx.doi.org/10.1021/ja2104944 | *J. Am. Chem.Soc.* 2012, 134, 2385−2391

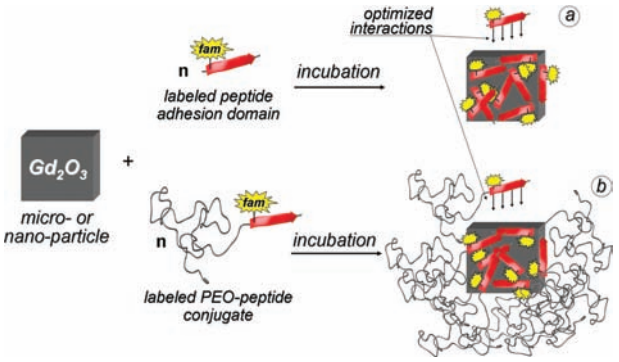

Figure 1. Schematic illustration of the peptide-mediated functionalization of inorganic particle surfaces by a tailor-made peptide adsorption domain, leading to either fluorescently marked functional particles (a) or PEO-shielded "stealthy" particles (b).

adhere specifically to well-defined inorganic or polymeric surfaces.[48,50−52] Pioneering studies from Sarikaya et al. as well as Belcher et al. demonstrated the potentials of the biocombinatorial tool. For instance, peptides could be selected that strongly and specifically adhere to single-crystal semiconductors.[47] Spectacularly, peptide binding discriminates between GaAs and AlGaAs despite similar crystal morphology and practically identical lattice constants of 5.66 Å and 5.65 Å, respectively. Meanwhile, several peptides were selected for example to specifically adhere to vaterite, calcite, or hydroxyapatite to act as morphology control additives in biomimetic crystallization.[48,49,53] Also peptides could be identified that effectively bind to polymeric surfaces and discriminate between iso- and syndiotactic poly(methyl methacrylate).[54]

Here, we describe the peptide-mediated functionalization of inorganic particle surfaces as a generalizable approach. The study exploits peptide adhesion domains for inorganic surfaces to introduce functionalities onto inorganic particles. The peptide sequences were selected by phage display methods and allow single-step coating procedures to render surfaces of inorganic particles either functional by introducing fluorescent probes or protein repellent by introducing poly(ethylene oxide).

RESULTS AND DISCUSSION

Gadolinium oxide (GdO) particles with monoclinic crystal morphology were used to demonstrate the feasibility of the approach (Supporting Information [SI], Figure S11). While a biomedical application is not in the focus of this material-based study, GdO NPs are of relevance as contrast agents for magnetic resonance imaging.[55,56] For ease of handling, submicrometer particles were obtained from commercial source particles by fractionated sedimentation. The average diameter of the GdO particles was found to be d_{SEM} = 590 ± 280 nm by scanning electron microscopy (SEM) (SI, Figure S7), and X-ray diffraction confirmed the monoclinic crystal morphology (SI, Figure S11). Brunauer−Emmett−Teller (BET) N_2-adsorption revealed accessible surfaces of ∼16.20 m^2/g. Comparing this value with ∼1.36 m^2/g that was calculated from d_{SEM} assuming compact spherical particles, indicated a rough surface topography. This was confirmed by transmission electron microscopy (SI, Figures S9,S10). In addition to core material, crystal morphology and topology, the surface stabilizers, which are permanently present on the particle surfaces, are highly relevant. The surface composition of nonmodified GdO particles was analyzed by X-ray photoelectron spectroscopy (XPS), providing background-corrected composition of 39.1 atom % carbon and 60.9 atom % oxygen. This corresponds well with ethylene glycol as nonionic stabilizer that is frequently used during particle synthesis. The bidental hydroxyl groups interact well with oxidic material surfaces, but allow for substitution by stronger binding entities via ligand exchange reactions. The overall amount of ethylene glycol compared to the bulk Gd_2O_3 is small as is evident from EDX (SI, Figure S14). Zeta potential measurements provide ζ = +30 mV, suggesting the absence of a dominant steric stabilization effect.

Phage display screening on GdO particles was performed as an affinity selection technique to determine strong peptide adhesion domains for the particular GdO surfaces. The screening process is referred to as biopanning and utilized phage display libraries of M13-bacteriophages.[57] The phages displayed a randomized dodecapeptide, which is exposed five times on the five pIII cap proteins of one side of the phage capsids. The library spans a sequential space of about 10^9 different peptides. Standard biopanning protocols were followed (cf. SI).[47,48] After five iterations of the biopanning, the peptide with the sequence NHWSDKRAQITI could be determined as strong binder for GdO particles. It should be noted, that usually 2−3 iterations are used, providing often a set of peptides with similar but not identical sequences. Probably it can be contributed to the fact that five iterations have been performed wherein practically only one sequence was found in six out of six sequenced codes. Accurate evaluation of point mutations indicated that, in total, two different phage clones were sequenced, displaying, however, the same binding sequence.

Phage display is a highly general method that reads out particle surfaces within an area of about 65 nm^2. In this process all local facets of the surfaces such as defects, morphology, charges, or roughness are taken into account and translate into a peptide sequence. Despite the fact that relationships between adhesion peptide sequences and material characteristics are still far from being understood, selected peptides will effectively bind even to surfaces of less defined particles or ill-defined technical products.

A set of peptides and poly(ethylene oxide)−peptide conjugates (PEO−peptide conjugates) was synthesized by solid-phase supported peptide synthesis (SPPS)[58] to investigate the properties of the adhesion domain. Additionally, appropriate peptide and PEO−peptide conjugate controls were synthesized, too. The controls exhibit statistically scrambled sequences of similar amino acid composition in order to elucidate the sequence specificity of peptide adsorption to GdO. All sequences were extended N-terminally by GG-inserts to space the relevant peptide segment from a carboxyfluorescein (fam) fluorescence label. Fam served as spectroscopic marker, enabling ease of analysis via fluorescence spectroscopy and microscopy.

After liberation of peptides and bioconjugates from the support, the fully deprotected products were isolated. The chemical structures of all compounds were confirmed by ESI- or MALDI-TOF mass spectrometry, FT-IR, and ^{1}H NMR (cf. SI). The following fam-labeled peptides were further investigated: fam-GG-NHWSDKRAQITI (AD* (labeled adhesion domain)) and fam-GG-DRINASHWQTIK (SC* (labeled scrambled domain)). The following bioconjugates with $M_{n,PEO}$

dx.doi.org/10.1021/ja2104944 | J. Am. Chem.Soc. 2012, 134, 2385−2391

= 3200 were investigated: fam-GG-NHWSDKRAQITI-*block*-PEO_{72} (PEO-AD*), fam-GG-DRINASHWQTIK-*block*-PEO_{72} (PEO-SC*), and fam-GG-*block*-PEO_{72} (PEO-GG*).

The function of the adhesion domain (AD*) was preliminarily evaluated by qualitative incubation experiments, indicating a significant surface modification compared to that of the controls. For that purpose, 2 mg GdO particles were incubated for 4 h in 0.5 mM aqueous stock solutions of the different peptides (AD*, SC*) or bioconjugates (PEO-AD*, PEO-SC*, PEO-GG*). After 10 careful washing steps the particles were dried, and energy-dispersive X-ray spectroscopy (EDX) was used to evaluate the changes in elemental composition compared to that of the nonmodified GdO particles (SI, Figure S14). EDX data indicated a significant increase of carbon to oxygen ratio (atom percent C/O) for the GdO_{AD*} (C/O = 0.25 ± 0.01) and the $GdO_{PEO\text{-}AD*}$ (C/O = 0.43 ± 0.05) compared to pure GdO particles (C/O = 0.00 ± 0.01). The significant increase in carbon content suggested qualitatively a surface modification by peptide-mediated functionalization. $GdO_{PEO\text{-}GG*}$, GdO_{SC*}, and $GdO_{PEO\text{-}SC*}$ showed only a slight increase of C/O ratio to 0.00 ± 0.02, 0.04 ± 0.01, and 0.05 ± 0.04, respectively.

The change in surface properties was also confirmed by contact angle measurements of water on glass slides, which were homogeneously covered with either modified or non-modified GdO particles. While the pure GdO had a static contact angle of 142.2°, the $GdO_{PEO\text{-}AD*}$ indicated a contact angle of 31.9° (SI, Figure S17). This suggested an effective surface modification of the GdO particles by peptide-mediated functionalization. Moreover, the hydrophobicity of the GdO particle surfaces was not dramatically changed when incubated with the controls (PEO-SC*, PEO-GG*). This reveals first hints of a sequence specificity of the peptide interactions with GdO.

The primary incubation experiments indicated an effective particle surface functionalization. A more detailed analysis of the peptide-mediated functionalization process required quantification of the peptide adsorption onto GdO. Initial adsorption of the different peptides onto GdO particles and reversibility of the particle coating were studied in a set of adsorption/elution experiments (Figure 2). Coating was performed by incubating 2 mg GdO in 0.5 mM aqueous peptide or bioconjugate stock solutions. After 4 h equilibration, the decrease in concentration of the stock solution could be followed by spectroscopy and represented a direct measure for the initial adsorption. Coating stability was observed by successive elution experiments, analyzing the amount of peptides or bioconjugates that could be washed off from the modified particles within 10 repetitive washing cycles.

The cumulative adsorption/elution diagrams of the incubation−wash experiments were shown in Figure 2. Comparing the adsorption/elution behavior of the adhesion peptide AD* and the scrambled control SC* indicated that both peptides adhered initially to the GdO particles (Figure 2A). Where AD* showed under the given conditions an adsorption of nearly 57% of the stock solution, only 41% of SC* was found to initially adhere during the incubation step. The high initial amounts of adhering peptides suggested a multilayer formation, which can be attributed to peptide−peptide interactions. More importantly, 13% of AD* remained irreversibly bound to the particles after 10 intense washing cycles, while practically all SC* could be eluted. Therefore, to 1 g of GdO particles, 60 mg of AD* were strongly bound, whereas no detectable SC* remained

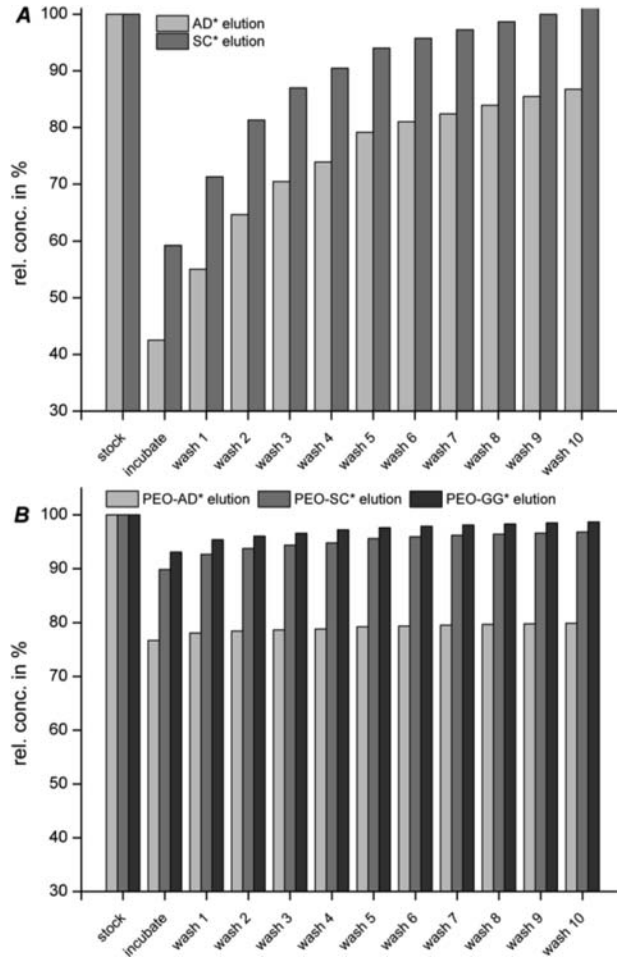

Figure 2. Cumulative adsorption/elution diagrams of (A) peptides and (B) bioconjugates. Peptides or bioconjugates were initially adsorbed to GdO in a primary incubation step. The concentration differences in the supernatant correspond to the initially adsorbed amounts. Sequential washing of the modified GdO particles elutes substances from the coating, which was plotted cumulatively and compared to the overall amount of applied substances. The differences indicated irreversible adsorbed substances.

after washing. The results indicated that peptide adsorption behavior depends strongly on the amino acid sequence. Despite the high energy surfaces of GdO, a sequential selectivity of the peptide-mediated functionalization process is evident. The difference in coating efficiency was confirmed by confocal fluorescence microscopy (Figure 3). Under similar conditions, the AD*-coated particles show a clear fluorescence signal, indicating a successful peptide-mediated functionalization of GdO with the fluorescence probe. As all of the scrambled peptides were practically washed off, no significant fluorescence could be found with the SC*-coated particles. This was consistent with the EDX investigations and confirmed that not only the amino acids but also the correct sequence is required to mediate effective adhesion onto GdO.

Careful analysis of the functionality and sequence of the selected adhesion domain (AD*) reveals several characteristics, which occur rather typically to binders for oxidic surfaces. The requirements to adhere to polar GdO surfaces are reflected by nine functional amino acids out of a 12*mer* sequence. Several cationic side-chain functionalities from His, Trp, Lys, and Arg are evident. In the middle of the sequence one Asp residue

dx.doi.org/10.1021/ja2104944 | *J. Am. Chem.Soc.* 2012, 134, 2385−2391

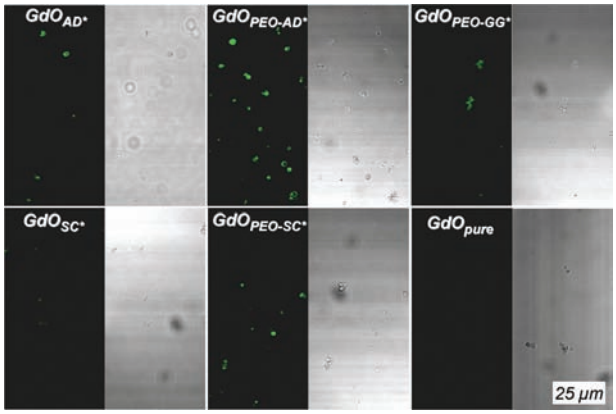

Figure 3. Fluorescence (left) and optical (right) microscopy images of surface-modified GdO particles after incubation and washing. While AD* and PEO-AD* result in particles with the most intense fluorescence, SC*-modified particles show none, and PEO-SC*, PEO-GG* show only weak, inhomogeneous fluorescence.

presents an anionically charged carboxylate. Additionally, polar H-bond capabilities are provided by Ser and Thr with β-hydroxyl groups as well as by Asn and Gln with primary amide groups. The C-terminal part of the sequence includes two Ile residues, which might lead to a slightly amphipathic character. Certainly the amino acid sequence is not random. Two distinct binding motifs might be discussed. As core motif the zwitterionic triad of DKR might lead to strong Coulombic binding interactions,[59] and C-terminally the ITI motif might be prone to strong entropically driven H-bonding.[60] It should be noted, that the findings are counterintuitive as the ζ-potential of the GdO particles shows positive surface charges. This reflects the potential of phage display as a tool to read out local surface properties at the nano scale.

The coating of inorganic particles with a PEO-shell is of tremendous importance for biomedical applications.[61] PEO suppresses effectively the primary protein adsorption and generates "stealthy" particles with increased biocompatibility, bioavailability, and reduced immunogenicity.[62,63] Therefore, the peptide-mediated functionalization of GdO particles with PEO−peptide conjugates was investigated. In a set of adsorption/elution experiments, PEO-AD* was compared with PEO-SC* and PEO-GG* controls. Figure 2B shows the corresponding adsorption/elution diagrams. As expected, PEO had a pronounced effect on the adsorption behavior. PEO-AD* adsorbed initially with 23% of the total amount of the stock solution and 20% remained irreversibly adhered after washing. With ∼250 mg PEO-AD* per gram GdO a significant coating has been obtained. The control PEO-SC* adhered with 10% initially, and only 3% remained irreversibly bound on the particles. This is straightforward to understand, as PEO conjugation to peptides or proteins reduces effectively "non-specific" interactions,[62] which downregulates the adsorption of PEO-SC* compared to that of PEO-AD*. Moreover, the adhesion of a PEO−peptide conjugate decorates the GdO surfaces with PEO. This prevents multilayer adsorption of additional bioconjugates in contrast to the adsorption of nonconjugated peptides. The PEO-GG* control shows with less than 1% irreversible residual after washing no obvious adsorption to GdO, confirming that neither fam-dye nor PEO have significant contribution to the adsorption behavior of PEO-AD*. Furthermore, an α-amino-ω-carboxyl-functional PEO (H_2N-PEO_{68}−COOH) was investigated as control to exclude an adsorption mediation via chain end-group functionalities. A nearly quantitative elution (99%) could be achieved already after three successive washing steps in standardized adsorption/elution experiments (SI, Figure S12).

The surface coverage of the peptide or the bioconjugate onto the GdO particles can be calculated. Considering the surface area of 16.20 m^2 per gram GdO as determined by N_2-adsorption and assuming peptides to adopt fully extended all-*trans* conformation with widths of 0.4 nm and lengths of 0.35 nm per amino acid residue (SI, Figure S18). This led to a coverage of ∼200% in the case of AD* and ∼310% in the case of the PEO-AD*. These values correspond to two and three monolayers on the particle surfaces, respectively (SI, Table S2). The occurrence of true, stable multilayers is certainly less likely. Alternatively, the observations could be rationalized by the fact that peptides adopt a random coil structure. This was confirmed by circular dichroism spectroscopy, indicating a statistical chain segment conformation of both peptides in AD* and PEO-AD*. Thus, a smaller contact area per molecule can be anticipated, which probably leads to monolayer surface occupation.

Fluorescence microscopy micrographs confirmed the modification of GdO particle surfaces by fluorescently labeled peptides and bioconjugates. Figure 3 qualitatively underlines the results of the adsorption/elution experiments. As expected, the most intense fluorescence signals are observed from GdO particles, which were modified by AD* and PEO-AD*. SC* modified particles show practically no fluorescence. PEO-SC*- or PEO-GG*-modified particles exhibit only weak fluorescence, as only ∼3% of the PEO-SC* and 0.5% of PEO-GG* adsorbed irreversibly to GdO particles. Apparently, the fluorescence of the PEO-SC*-modified particles is rather heterogeneous in nature compared to that of PEO-AD*-modified particles. Obviously, larger particles occurring in the optical microscopy image show only very weak fluorescence (SI, Figure S16).

Binding assays were performed with systematically altered concentrations of peptides or bioconjugates. These allowed for the access of Langmuir adsorption constants (K_L), which are proportional to the rate constants of adsorption to surfaces of the GdO particles and reflect the binding energies. Langmuir constants between 10^4 and 10^6 M^{-1} are frequently observed for surface interactions of 12*mer* peptides.[54,64] Kinetic adsorption studies applied the model of Langmuir isotherm (Figure 4) and revealed the specificity of the interactions of peptides or bioconjugates. K_L was determined to be 0.12×10^5 M^{-1} for AD*, 0.00×10^5 M^{-1} for SC*, 0.98×10^5 M^{-1} for PEO-AD*, and 0.04×10^5 M^{-1} for PEO-SC*. Qualitatively, these data agreed well with the results of the adsorption/elution experiments and underlined the differences in coating stabilities.

The isotherms clearly highlighted the importance of the peptide sequence on the adsorption behavior. Most evident were differences between the nonconjugated peptides, as PEO was not modulating differences in adsorption behavior. K_L for AD* was significantly increased, compared to that of SC*, suggesting a high binding energy difference as a result of the different peptide sequences. The K_L for SC* was almost zero reflecting a low adsorption and a strong desorption tendency. A similar tendency was observed for the PEO−peptide conjugates, where K_L was ∼25-fold higher for PEO-AD* compared to that of the scrambled analogue PEO-SC*.

The effect of the conjugated PEO appears to be highly interesting. Obviously, PEO introduction to both peptides

dx.doi.org/10.1021/ja2104944 | J. Am. Chem.Soc. 2012, 134, 2385−2391

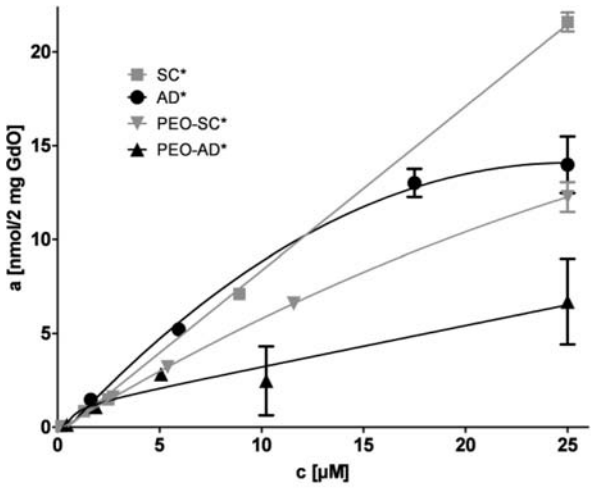

Figure 4. Langmuir isotherms of AD*, PEO-AD*, SC*, and PEO-SC*. GdO particles were incubated with aqueous solutions of the different substances at various concentrations (c). The amount of adsorbed substance (a) was estimated by spectroscopic means, measuring the decrease of the substance concentrations in supernatants.

(AD* and SC*) resulted in a strong increase of the corresponding K_L values. Probably, this could be rationalized by reduction of conformational flexibility of the peptide segments, which might drive surface adhesion tendency by a reduced entropic penalty. Alternatively, PEO can suppress peptide−peptide interactions in solution, shifting the solution equilibrium from transient aggregates toward unimers. The latter would be more likely to exhibit higher binding energies as compared to peptide aggregates. A remarkable increase in adsorption selectivity was obtained by the introduction of PEO. This was evident by a significantly smaller difference between the K_L values of SC* and AD* as compared to that between those of PEO-SC* and PEO-AD*. This was expected as PEO introduction for example to proteins reduces nonspecific interactions.[62] Hence, the PEO-block assists to optimize surface binding of the peptide adhesion domain and reduces nonoptimal binding events.

Size-dependent adsorption effects are described for protein−particle interactions, showing often interesting relationships.[65,66] To exclude dominant effects, the adsorption of PEO-AD* onto GdO particles with three different mean diameters ($d(GdO_{(s)})$ = 250 ± 125 nm, $d(GdO_{(m)})$ = 590 ± 200 nm, and $d(GdO_{(l)})$ = 4 ± 2 μm (SI, Figures S8, S7, and S6, respectively) have been studied. The dependence of adsorption capacities on particle size was investigated by performing standardized adsorption/elution experiments. The results have been consistent and do not indicate abnormal behavior of PEO-AD* adhesion or coating stability, within the analyzed particle size window (SI, Figure S13 and Table S1). Where large GdO particles could be coated with 90 mg bioconjugate per gram GdO (adsorption capacity 7% under standardized conditions), medium particles show 260 mg PEO-AD* coating per gram GdO and the small particles lead to stable coatings of 510 mg PEO-AD* per gram GdO. The trend clearly shows an increase in adsorption capacity with increased surface area (decreased particle size). Focusing on the two smallest particle sizes, where size-dependent adsorption would be most evident, a normalized ratio (μmol (PEO-AD*) per m^2 of GdO surface) meets within the experimental error comparable to values of 32 μmol/m^2 (small) and 35 μmol/m^2 (medium).

To ultimately demonstrate the relevance of the noncovalent coating of inorganic particles via peptide-mediated functionalization, initial protein adsorption experiments have been carried out. Adsorption of rhodamine-marked bovine serum albumin (BSA*) onto GdO particles ($GdO_{(m)}$) was investigated. BSA is known to bind rapidly to oxidic and/or hydrophobic surfaces.[67] Dense PEO coatings of diverse surfaces (often referred to as PEGylation) reduces protein−surface interactions and produces "stealthy" surfaces.[68,69] The effect of the surface modification was investigated by incubating PEO-AD*- and PEO-SC*-modified GdO particles as well as nonmodified GdO particles with a 0.63 μmol stock solution of fluorescently labeled BSA* (SI, Figure S19).[70] As expected, nonmodified GdO particles showed considerable adsorption of BSA*, decreasing the stock concentration by about 92%. Also PEO-SC* was not resulting in an effective coating of GdO particles, as 72% of the BSA* adsorbed onto the particles. In contrast to this, the coated $GdO_{PEO\text{-}AD*}$ particles adsorbed only 12% of BSA*. Obviously, the PEO coating reduced the capacity of protein adsorption by about 80%. This suggests a distinct shielding effect. Remarkably, the coating is stable enough not to be prone to ligand-exchange reactions as no obvious substitution of surface-bound PEO-AD* by BSA* was observed overnight.

CONCLUSION

The concept of peptide-mediated functionalization of inorganic nanoparticles was demonstrated on submicrometer gadolinium oxide (GdO) particles. Phage display was used to select appropriate dodecapeptides, which adhere to surfaces of GdO particles. The peptide adhesion domains interacted strongly with GdO particles, and sequence selectivity was revealed by comparison with peptide controls, which have a scrambled amino acid sequence. The noncovalent decoration of GdO particles allowed the straightforward functionalization of the surfaces with fluorescence labels or poly(ethylene oxide) (PEO). On the one hand the particles were marked fluorescently as proven by fluorescence microscopy. On the other hand the particle surface was modified from hydrophobic to hydrophilic. Surface modification was shown by energy-dispersive X-ray spectroscopy (EDX) and contact angle measurements, indicating a change in elemental composition and strong increase in wettability with water, respectively. Coating stability against washing was investigated by adsorption/elution experiments, showing that the adsorption domain strongly adhered to surfaces of GdO particles, whereas the scrambled peptide could be eluted by washing steps in a rather quantitative manner. Langmuir isotherms confirmed these experiments, by showing distinguishable adsorption coefficients. This highlighted the importance of the peptide sequence (adsorption domain versus scrambled peptide). Interestingly, the PEO-blocks of PEO−peptide conjugates regulated the adsorption effects, leading to a more specific formation of coated particles. Ultimately, peptide-mediated modification of GdO particles with PEO resulted in PEO-coated particles, which exhibit strongly reduced protein adsorption capacity. The latter might be of importance for biomedical applications. Despite the fact that the peptide-mediated functionalization was demonstrated on GdO particles, phage display technology has proven to be capable of selecting peptides, which strongly bind to various inorganic, organic,

dx.doi.org/10.1021/ja2104944 | J. Am. Chem.Soc. 2012, 134, 2385−2391

polymeric, and bioorganic surfaces. Hence, the procedure not only can provide surface engineering for gadolinium oxide nanoparticles as highly relevant MRI contrast agent for diagnostic applications but also provides the possibility to expand the single-step, noncovalent coating toward diversity of other functional particles. The establishment of a material surface-specific coating process might drive materials science applications from glues, to coatings, to formulation additives. Moreover, next-generation nanoengineering of particle surfaces might envision anisotropic decoration of nanoparticles. For instance, selected peptide adhesion domains might address specific regions of anisotropic rodlike nanoparticles or specific crystal faces of crystalline monodomain nanoparticles.

■ ASSOCIATED CONTENT

Supporting Information

Detailed experimental data, materials, and methods as well as synthesis protocols and analytics. This material is available free of charge via the Internet at http://pubs.acs.org.

■ AUTHOR INFORMATION

Corresponding Author

h.boerner@hu-berlin.de

■ ACKNOWLEDGMENTS

H.G.B. acknowledges financial support by the Center of Supramolecular Interactions Berlin (CSI Berlin), DFG (CORE BO1762/4-1, and BEKs BO1762/5-1). D.F.'s research is supported by the ERC (Project MB2, Starting Grant 256915) and the Max Planck Society. We acknowledge Prof. Rademann (HU-Berlin) for providing the possibility for ESEM and EDX, Prof. Thomas and Johannes Schmidt (TU-Berlin) for XRD and BET. We thank Prof. Friedrich (BAM, Berlin) for XPS measurements. André Körnig (MPIKG) is acknowledged for fluorescence microscopy.

■ REFERENCES

(1) Mirkin, C. A.; Letsinger, R. L.; Mucic, R. C.; Storhoff, J. J. *Nature* **1996**, *382*, 607−609.
(2) Zhao, Y.; Thorkelsson, K.; Mastroianni, A. J.; Schilling, T.; Luther, J. M.; Rancatore, B. J.; Matsunaga, K.; Jinnai, H.; Wu, Y.; Poulsen, D.; Fréchet, J. M. J.; Alivisatos, A. P.; Xu, T. *Nat. Mater.* **2009**, *8*, 979−985.
(3) De, M.; Ghosh, P. S.; Rotello, V. M. *Adv. Mater.* **2008**, *20*, 4225−4241.
(4) Lin, Y.; Boker, A.; He, J. B.; Sill, K.; Xiang, H. Q.; Abetz, C.; Li, X. F.; Wang, J.; Emrick, T.; Long, S.; Wang, Q.; Balazs, A.; Russell, T. P. *Nature* **2005**, *434*, 55−59.
(5) Burns, A.; Ow, H.; Wiesner, U. *Chem. Soc. Rev.* **2006**, *35*, 1028−1042.
(6) Suh, W. H.; Suslick, K. S.; Stucky, G. D.; Suh, Y. H. *Prog. Neurobiol.* **2009**, *87*, 133−170.
(7) Niederberger, M.; Cölfen, H. *Phys. Chem. Chem. Phys.* **2006**, *8*, 3271−3287.
(8) Weller, H. *Angew. Chem., Int. Ed.* **1993**, *32*, 41−53.
(9) Noginov, M. A.; Zhu, G.; Belgrave, A. M.; Bakker, R.; Shalaev, V. M.; Narimanov, E. E.; Stout, S.; Herz, E.; Suteewong, T.; Wiesner, U. *Nature* **2009**, *460*, 1110−1112.
(10) Kim, B. Y.; Shim, I. B.; Araci, Z. O.; Saavedra, S. S.; Monti, O. L. A.; Armstrong, N. R.; Sahoo, R.; Srivastava, D. N.; Pyun, J. *J. Am. Chem. Soc.* **2010**, *132*, 3234−3235.
(11) Lu, A. H.; Salabas, E. L.; Schuth, F. *Angew. Chem., Int. Ed.* **2007**, *46*, 1222−1244.
(12) Wong, S.; Kitaev, V.; Ozin, G. A. *J. Am. Chem. Soc.* **2003**, *125*, 15589−15598.
(13) Law, M.; Greene, L. E.; Johnson, J. C.; Saykally, R.; Yang, P. D. *Nat. Mater.* **2005**, *4*, 455−459.
(14) Kamat, P. V. *J. Phys. Chem. B* **2002**, *106*, 7729−7744.
(15) Shipway, A. N.; Katz, E.; Willner, I. *ChemPhysChem* **2000**, *1*, 18−52.
(16) Suh, W. H.; Suh, Y. H.; Stucky, G. D. *Nano Today* **2009**, *4*, 27−36.
(17) Rosi, N. L.; Mirkin, C. A. *Chem. Rev.* **2005**, *105*, 1547−1562.
(18) Saha, K.; Bajaj, B.; Duncan, B.; Rotello, V. M. *Small* **2011**, *7*, 1903−1918.
(19) Yin, Y.; Alivisatos, A. P. *Nature* **2005**, *437*, 664−670.
(20) Mirkin, C. A. *Inorg. Chem.* **2000**, *39*, 2258−2272.
(21) Sanchez, C.; Soler-Illia, G.; Ribot, F.; Lalot, T.; Mayer, C. R.; Cabuil, V. *Chem. Mater.* **2001**, *13*, 3061−3083.
(22) Peer, D.; Karp, J. M.; Hong, S.; Farokhzad, O. C.; Margalit, R.; Langer, R. *Nat. Nanotechnol.* **2007**, *2*, 751−760.
(23) Caruso, F.; Caruso, R. A.; Mohwald, H. *Science* **1998**, *282*, 1111−1114.
(24) Quaroni, L.; Chumanov, G. *J. Am. Chem. Soc.* **1999**, *121*, 10642−10643.
(25) Pyun, J. *Polym. Rev.* **2007**, *47*, 231−263.
(26) Charleux, B.; D'Agosto, F.; Delaittre, G. *Adv. Polym. Sci.* **2010**, *233*, 125−183.
(27) Darbandi, M.; Urban, G.; Kruger, M. *J. Colloid Interface Sci.* **2010**, *351*, 30−34.
(28) Chuang, F. Y.; Yang, S. M. *J. Colloid Interface Sci.* **2008**, *320*, 194−201.
(29) Bourgeat-Lami, E.; Lansalot, M. *Adv. Polym. Sci.* **2010**, *233*, 53−123.
(30) Daniel, M. C.; Astruc, D. *Chem. Rev.* **2004**, *104*, 293−346.
(31) Schlenoff, J. B.; Li, M.; Ly, H. *J. Am. Chem. Soc.* **1995**, *117*, 12528−12536.
(32) Vericat, C.; Vela, M. E.; Benitez, G.; Carro, P.; Salvarezza, R. C. *Chem. Soc. Rev.* **2010**, *39*, 1805−1834.
(33) Freeman, C. L.; Harding, J. H.; Quigley, D.; Rodger, P. M. *Angew. Chem., Int. Ed.* **2010**, *49*, 5135−5137.
(34) Beniash, E. *Wiley Interdiscip. Rev. - Nanomed. Nanobiotechnol.* **2011**, *3*, 47−69.
(35) Börner, H. G. *Prog. Polym. Sci.* **2009**, *34*, 811−851.
(36) Hest, J. C. M. v.; Tirrell, D. A. *Chem. Commun.* **2001**, 1897−1904.
(37) Heredia, K. L.; Maynard, H. D. *Org. Biomol. Chem.* **2007**, *5*, 45−53.
(38) Lutz, J.-F.; Börner, H. G. *Prog. Polym. Sci.* **2008**, *33*, 1−39.
(39) Börner, H. G. *Macromol. Rapid Commun.* **2011**, *32*, 115−126.
(40) Hartmann, L.; Börner, H. G. *Adv. Mater.* **2009**, *21*, 3425−3431.
(41) Sarikaya, M.; Tamerler, C.; Jen, A. K. Y.; Schulten, K.; Baneyx, F. *Nat. Mater.* **2003**, *2*, 577−585.
(42) Tomczak, M. M.; Glawe, D. D.; Drummy, L. F.; Lawrence, C. G.; Stone, M. O.; Perry, C. C.; Pochan, D. J.; Deming, T. J.; Naik, R. R. *J. Am. Chem. Soc.* **2005**, *127*, 12577−12582.
(43) Wang, T.; Mitchell, J.; Börner, H.; Cölfen, H.; Antonietti, M. *Phys. Chem. Chem. Phys.* **2010**, *12*, 11984−11992.
(44) Page, M. G.; Nassif, N.; Börner, H. G.; Antonietti, M.; Cölfen, H. *Cryst. Growth Des.* **2008**, *8*, 1792−1794.
(45) Tamerler, C.; Khatayevich, D.; Gungormus, M.; Kacar, T.; Oren, E. E.; Hnilova, M.; Sarikaya, M. *Biopolymers* **2010**, *94*, 78−94.
(46) Tamerler, C.; Sarikaya, M. *Acta Biomater.* **2007**, *3*, 289−299.
(47) Whaley, S. R.; English, D. S.; Hu, E. L.; Barbara, P. F.; Belcher, A. M. *Nature* **2000**, *405*, 665−668.
(48) Roy, M. D.; Stanley, S. K.; Amis, E. J.; Becker, M. L. *Adv. Mater.* **2008**, *20*, 1830−1836.
(49) Sarikaya, M.; Tamerler, C.; Schwartz, D.; Baneyx, F. *Annu. Rev. Mater. Res.* **2004**, *34*, 373−408.
(50) Kase, D.; Kulp, J. L.; Yudasaka, M.; Evans, J. S.; Iijima, S.; Shiba, K. *Langmuir* **2004**, *20*, 8939−8941.
(51) So, C. R.; Kulp, J. L.; Oren, E. E.; Zareie, H.; Tamerler, C.; Evans, J. S.; Sarikaya, M. *ACS Nano* **2009**, *3*, 1525−1531.

(52) Weiger, M. C.; Park, J. J.; Roy, M. D.; Stafford, C. M.; Karim, A.; Becker, M. L. *Biomaterials* **2010**, *31*, 2955−2963.
(53) Gebauer, D.; Verch, A.; Börner, H. G.; Cölfen, H. *Cryst. Growth Des.* **2009**, *9*, 2398−2403.
(54) Serizawa, T.; Matsuno, H.; Sawada, T. *J. Mater. Chem.* **2011**, *21*, 10252−10260.
(55) Bridot, J. L.; Faure, A. C.; Laurent, S.; Rivière, C.; Billotey, C.; Hiba, B.; Janier, M.; Josserand, V.; Coll, J. L.; Elst, L. V.; Muller, R.; Roux, S.; Perriat, P.; Tillement, O. *J. Am. Chem. Soc.* **2007**, *129*, 5076−5084.
(56) Na, H. B.; Song, I. C.; Hyeon, T. *Adv. Mater.* **2009**, *21*, 2133−2148.
(57) Kehoe, J. W.; Kay, B. K. *Chem. Rev.* **2005**, *105*, 4056−4072.
(58) Eckhardt, D.; Groenewolt, M.; Krause, E.; Börner, H. G. *Chem. Commun.* **2005**, 2814−2816.
(59) Page, M. G.; Nassif, N.; Börner, H. G.; Antonietti, M.; Cölfen, H. *Cryst. Growth Des.* **2008**, *8*, 1792−1794.
(60) Kessel, S.; Börner, H. G. *Macromol. Rapid Commun.* **2008**, *29*, 419−424.
(61) Otsuka, H.; Nagasaki, Y.; Kataoka, K. *Adv. Drug. Delivery Rev.* **2003**, *55*, 403−419.
(62) Alconcel, S. N. S.; Baas, A. S.; Maynard, H. D. *Polym. Chem.* **2011**, *2*, 1442−1448.
(63) Knop, K.; Hoogenboom, R.; Fischer, D.; Schubert, U. S. *Angew. Chem., Int. Ed.* **2010**, *36*, 6288−6308.
(64) Sano, K.-I.; Sasaki, H.; Shiba, K. *Langmuir* **2005**, *21*, 3090−3095.
(65) Lundqvist, M.; Sethson, I.; Jonsson, B. H. *Langmuir* **2004**, *20*, 10639−10647.
(66) Wang, D. W.; Nap, R. J.; Lagzi, I.; Kowalczyk, B.; Han, S. B.; Grzybowski, B. A.; Szleifer, I. *J. Am. Chem. Soc.* **2011**, *133*, 2192−2197.
(67) Müller, B.; Zacharias, M.; Rezwan, K. *Adv. Eng. Mater.* **2010**, *12*, B53−B61.
(68) Prime, K. L.; Whitesides, G. M. *J. Am. Chem. Soc.* **1993**, *115*, 10714−10721.
(69) Chapman, R. G.; Ostuni, E.; Takayama, S.; Holmlin, R. E.; Yan, L.; Whitesides, G. M. *J. Am. Chem. Soc.* **2000**, *122*, 8303−8304.
(70) Cai, H.-H.; Zhong, X.; Yang, P.-H.; Wei, W.; Chen, J.; Cai, J. *Colloids Surf., A* **2010**, *372*, 35−40.